Multichannel Photon-Pair Generation with Strong and Uniform Spectral Correlation in a Silicon Microring Resonator

Xiaodong Shi,[1] Kai Guo,[2,*] Jesper Bjerge Christensen,[1] Mario A. Usuga Castaneda,[1] Xuanming Liu,[2] Haiyan Ou,[1] and Karsten Rottwitt[1]

[1]*Department of Photonics Engineering, Technical University of Denmark, Kongens Lyngby 2800, Denmark*
[2]*Institute of Systems Engineering, AMS, Beijing 100039, China*

We experimentally demonstrate a photon-pair source, based on continuous-wave pumped spontaneous four-wave mixing in a silicon microring resonator, which efficiently generates photon pairs with high coincidence counts, high brightness, and high coincidence-to-accidental ratio at multiple resonance wavelengths matching a standard International Telecommunication Union (ITU) frequency grid. The signal-idler joint spectral intensity is measured with a very high resolution of 2 pm over multiple wavelengths by an optical spectrum analyzer through probe-swept stimulated four-wave mixing, allowing an accurate quantification of the spectral correlation. Strong spectral correlation and uniform degree of quantum correlation are observed from the source, and the measured amount of spectral modes agrees well with that obtained by unheralded second-order correlation measurements.

I. INTRODUCTION

Quantum photonics holds great promise within modern optical information processing, with applications ranging from quantum computing, quantum spectroscopy, and quantum imaging to quantum communication [1–4]. In high-security quantum communication, the entanglement of photons, involving polarization, time bin, or time energy as degrees of freedom, is to be employed as the information carriers [5–7]. Time-energy entanglement, requiring spectral correlation, possesses the superiority of low propagation loss and small group-velocity dispersion in single-mode optical fibers, which benefits long-haul quantum key distribution (QKD), compared to the use of polarization entanglement or spatial entanglement [7,8]. Hence, high-quality photon-pair sources, characterized by high coincidence counts, high brightness, high coincidence-to-accidental ratio (R_{CA}), and strong spectral correlation, are highly desirable. Moreover, wavelength-division multiplexing (WDM), with low cross talk, is effective for dense channel spacing [9], which enables parallel distribution of photon pairs at multiwavelength channels, and to reroute the correlated photon pairs to accommodate multiple users, extending the information capacity of quantum networks [10–12].

As a CMOS compatible material, silicon is extensively used for on-chip photon-pair sources via spontaneous four-wave mixing (SpFWM), due to the mature fabrication procedure, low cost, and high material-based third-order nonlinear susceptibility [13–15]. By taking advantage of the high nonlinear refractive index and the submicron-scale cross sections, silicon waveguides enable tight mode confinement and high nonlinearity [16]. Furthermore, by applying a continuous-wave (CW) laser as the pump to silicon waveguides, both broadband SpFWM and strong spectral correlation can be achieved, allowing efficient time-energy entanglement [17]. To generate photon pairs in an ultrasmall footprint for compact integrated functionality, microring resonators have proven to be extremely suitable [13,18]. Recently, a silicon microring photon pair source with measured coincidence counts of 4869 Hz and R_{CA} of 1.2×10^4, using efficient superconducting nanowire single-photon detectors, has been reported [14]. Light at the resonance wavelengths is enhanced in the cavity, reinforcing nonlinear interaction, which can be regarded as a narrow multi-band-pass filter, leading to much higher spectral brightness compared to straight waveguides [19]. The free spectral range (FSR) of the microring is given by $\Delta\lambda_{FSR} = \lambda^2/(n_g L)$, where L is the microring circumference and n_g is the group velocity refractive index in the cavity [20]. Therefore, by carefully designing the resonator size, it is possible to make the FSR match the standard International Telecommunication Union (ITU) frequency grid and thereby enable multichannel photon-pair generation to be compatible with commercial WDM devices, such as arrayed waveguide gratings (AWG).

The spectral correlation of photon pairs can be characterized by reconstructing the signal-idler joint

---

spectral intensity (JSI). The JSI indicates the detected photon-pair probability distribution in the frequency domain, depicted by the idler wavelength as a function of signal wavelength [21]. Both quantum and classical methods have been reported to build up the JSI [22–27].

On the one hand, the quantum method is not suitable for the microring resonator with a high quality factor, because few optical components provide picometer bandwidth filtering. On the other hand, the classical method has been experimentally proved to be efficient and highly resolved, with high signal-to-noise ratio in straight waveguides [24]. A fixed pump laser and a tunable narrow-linewidth laser, scanning within the signal spectral range, are used to generate stimulated four-wave mixing (StFWM), and an optical spectrum analyzer (OSA) or a spectrometer is applied to measure the idler spectrum. Recently, the classical method was used to construct the JSI of a microring source with a resolution of 5 pm, using a Fabry-Perot interferometer that was stabilized by a reference laser and a spectrometer that was coupled to a CCD camera for detection [25]. However, the classical method using high-spectral-resolution OSAs has not been reported before for measuring the JSI of a wavelength-multiplexed microring photon-pair source.

In this work, we first measure the coincidence counts, brightness, and R_{CA} of our wavelength-multiplexed system. Then, we characterize the spectral correlation of the photon pairs by reconstructing a highly resolved JSI using the classical method and compare the results with the measurement of the unheralded second-order correlation function.

II. PHOTON-PAIR GENERATION MEASUREMENT

A schematic of the experimental setup for photon-pair generation is shown in Fig. 1(a). The pump, a CW laser (ANDO AQ4321D) at 1554.75 nm, is amplified to 25 dBm by an erbium-doped fiber amplifier (EDFA). The pump light passes through multiple tunable band-pass filters (TBPFs) to filter out the pump sideband noise and amplified spontaneous emission noise arising from the EDFA. A variable attenuator (ATT) and a polarization controller (PC) are used to adjust the pump power and to maximize the coupling efficiency for the transverse electric (TE) polarization, respectively. The pump is coupled in and out of the waveguide using a pair of photonic crystal grating couplers with a 3-dB transmission bandwidth of 29 nm, by means of single-mode fibers held by 15° vertical holders [28]. The chip is put on a stage, connected to a temperature controller. Three cascaded AWGs, with a dense channel spacing of 200 GHz, band isolation of 120 dB, and narrow full width at half maximum (FWHM) transmission bandwidth of 0.4 nm, are employed to demultiplex photon pairs into multiple channels and reduce the noise,
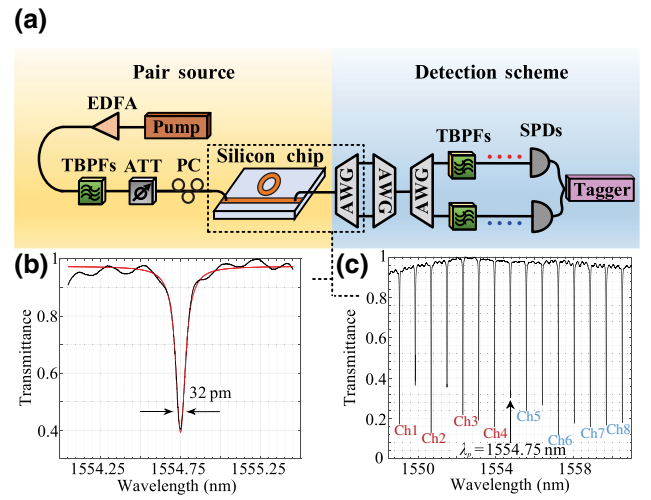

FIG. 1. (a) Experimental setup for photon-pair generation. (b) The transmittance at pump wavelength of 1554.75 nm, with a FWHM of 32 pm. (c) The transmittance that exactly matches the 200-GHz AWG channels (Ch1–Ch8).

including pump leakage and spontaneous Raman scattering noise, down to −140 dBm. The selected photons in the signal and idler channels are then launched to two free-running single-photon detectors (SPDs, ID230, ID Quantique), with a dark count rate of 50 Hz, collection efficiency of 20%, and deadtime of 10 μs. To record coincidental-temporal histograms, the two SPDs are connected to a time-tagging unit (ID801) with a time bin of 81 ps.

We fabricate the microring resonator on a SOI wafer with a 250-nm top silicon layer and a 3-μm buried silica layer. A 1-μm-thick silica layer is deposited as cladding. The microring is all-pass type, where the gap between the bus waveguide and the loop is 120 nm. The cross-sectional dimension of the silicon core is $H \times W = 250 \times 430$ nm, with a group refractive index $n_g \approx 4.3$ at 1550 nm. The waveguide design makes the near-zero anomalous dispersion range cover the entire ITU grid from 1528 to 1564 nm. The ring radius is designed to be 110 μm, corresponding to a FSR of $\nu_{FSR} \approx 100$ GHz, matching the standard ITU frequency grid. Figure 1(b) depicts the measured transmission spectrum at the pump wavelength of 1554.75 nm and the fitted transmission spectrum made by the Lorentzian function, presenting a FWHM of 32 pm, which indicates a quality factor Q of approximately 5×10^4. The resonant wavelength separation of the microring resonator can be designed by the radius of the microring, but the resonant wavelength cannot be controlled to exactly match the wavelength of the AWG channels, due to the fabrication fluctuation. A temperature controller is used to change the temperature of the chip, so that the resonant wavelength of the microring resonator can be tuned. Meanwhile, it is also used to avoid the resonance drift during the experiment [29]. The power of the temperature controller is around

50 W. As shown in Fig. 1(c), the central wavelengths of the signal-idler photon pairs are 1549.2 and 1560.4 nm, 1550.8 and 1558.8 nm, 1552.4 and 1557.2 nm, and 1554.0 and 1555.6 nm, matching exactly with channel 1 (Ch1) and channel 8 (Ch8), channel 2 (Ch2) and channel 7 (Ch7), channel 3 (Ch3) and channel 6 (Ch6), and channel 4 (Ch4) and channel 5 (Ch5) of the AWGs that we use, respectively.

The coincidence counts and the R_{CA} are measured at different incident power levels, by adjusting the variable attenuator to keep a constant optical SNR of the pump. We focus on the photon-pair generation and demultiplexing at three resonance pairs, Ch1–Ch8, Ch2–Ch7, and Ch3–Ch6, with distinct coincidence peaks in the coincidental-temporal histograms. It is noticed that the photon-pair generation in Ch4–Ch5 cannot be detected, since the coincidence peak is hidden in the accidental coincidence background, due to the high incident pump sideband noise. The coincidence peak in the histogram obtained from the time-tagging unit, presenting the raw coincidence counts (R_{cc}), is jointly composed of the true coincidence counts contributed by photon pairs and the accidental coincidence counts contributed by noise. Therefore, the R_{CA} is calculated as $R_{\mathrm{CA}} = (R_{\mathrm{cc}} - A_{\mathrm{cc}})/A_{\mathrm{cc}}$, where A_{cc} denotes the average background accidental counts in the coincidental-temporal histogram. The pair brightness is given by $B = R_{\mathrm{cc}}/(\Delta t P_p \Delta \lambda_{\mathrm{res}})$, where Δt is measurement time, P_p is pump power, and $\Delta \lambda_{\mathrm{res}}$ is the FWHM of the wavelength channel.

Figure 2 shows the coincidence counts and the R_{CA} versus the input pump power per minute for Ch1–Ch8, Ch2–Ch7, and Ch3–Ch6. It is noticed that the measurement is operated far below the threshold of the parametric oscillation, approximately 34 mW, based on $P_{\mathrm{th}} \approx 1.54 \pi Q_e n^2 L A_{\mathrm{eff}}/4 n_2 \lambda_p Q^3$, where Q_e is the external quality factor, L is the round trip length of the mircoring, A_{eff} is the effective mode area, and n_2 is the nonlinear refractive index [30]. The maximal coincidence counts and the highest R_{CA} of Ch1–Ch8, Ch2–Ch7, and Ch3–Ch6 are 33 Hz and 468, 30 Hz and 284, and 20 Hz and 132, respectively. The pair brightness is calculated to be 694, 504, and

329 (s mW nm)$^{-1}$ for the maximal coincidence counts in the three resonance pairs. The brightness of the microring is 2 orders of magnitude higher than that of the straight waveguide [15].

At pump power levels below 0.5 mW, the coincidence counts of three resonance pairs fit well to a quadratic dependence in pump power, indicating that the photon pairs generated by SpFWM are dominant in all coincidence events [31]. However, as the pump power is increased, the coincidence counts start to saturate, which is caused by both the onset of nonlinear loss and the detector saturation [18]. The maximal coincidence counts that are achieved with only nonlinear loss are 527, 231, and 74 Hz for Ch1–Ch8, Ch2–Ch7, and Ch3–Ch6, respectively. The R_{CA} decreases in general with increasing pump power, because the multi-photon-pair generation is promoted at a high pump-power level. Our SPDs operate in a free-running regime, so that high accidental counts could restrict the detection of true coincidence counts. As the photon-pair generation by SpFWM is a probabilistic event, and the single-photon-pair generation and multi-photon-pair generation are coupled to each other [13], there is no shortcut to acquire both large coincidence counts, contributed by single-photon-pair generation, and high R_{CA}, restrained by multi-photon-pair generation, simultaneously. These measurements are limited by the low speed and efficiency of the (In, Ga)As/InP avalanche photodiodes. This can be improved by utilizing superconducting SPDs instead, with high detection rate, low dark count, near-unity efficiency, and short deadtime. Furthermore, the pump sideband noise decreases with increasing wavelength separation between the photon pairs. This is explained by of the Gaussian-shaped transmittance of the TBPFs, resulting in the increasing R_{CA}. Meanwhile, the channels with narrow separation are closer to the pump wavelength, containing a larger amount of pump sideband noise photons. Such noise photons affect the effective coincidental photon detection of the SPDs, leading to low coincidence counts and low R_{CA}. Therefore, given that silicon waveguides provide a broad SpFWM bandwidth (36 nm in
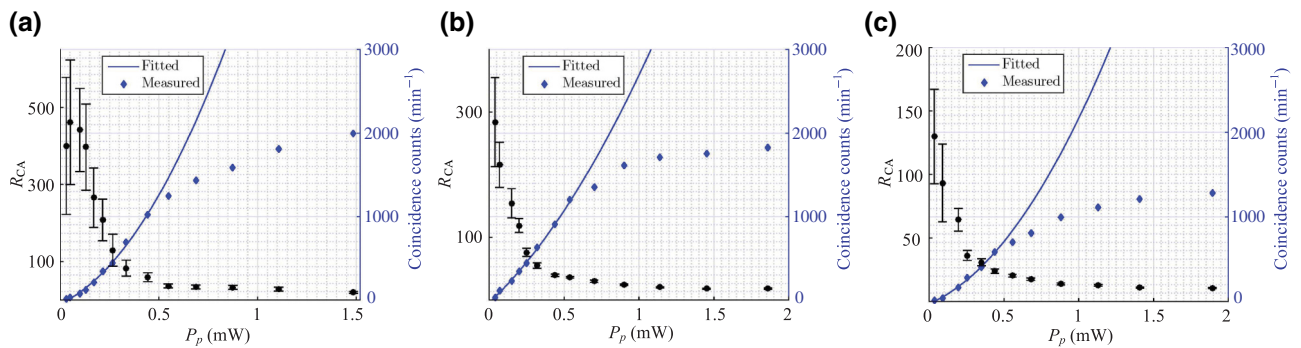

FIG. 2. The measured coincidence counts (blue) and the R_{CA} (black) versus pump power in bus waveguide per minute, for (a) Ch1–Ch8, (b) Ch2–Ch7, and (c) Ch3–Ch6.
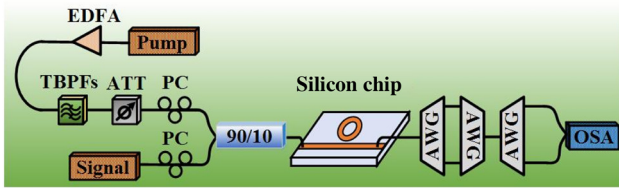
FIG. 3. Experimental setup for JSI measurement. 90/10 denotes the 90%/10% coupler.

our case calculated through the method in Ref. [32]), it is inferred that the performance should be even better for the photon pairs of wider wavelength separation.

III. SPECTRAL CORRELATION MEASUREMENT

A schematic of the experimental setup for the JSI reconstruction through probe-swept stimulated four-wave mixing is shown in Fig. 3. In the measurement, the input pump power in the bus waveguide is kept at 18 dBm, which is above the threshold of the parametric oscillation, while the tunable CW signal seed is at -15 dBm. The wavelength of the signal laser is tuned in a range of 240 pm, with a step of 2 pm, centered at every signal resonance of the microring. Passing through a PC, the signal seed is combined with the pump by a 90%/10% coupler and coupled to the waveguide. After the cascaded AWG system, the corresponding idler spectrum is swept by an OSA (ANDO AQ6317B), with a spectral resolution of 2 pm. We measure the JSI, with a 120-by-120 pixel grid having a resolution of 2 pm per pixel, choosing Ch1, Ch2, and Ch3 as the signal channels and Ch6, Ch7, and Ch8 as the corresponding idler channels, respectively.

Figure 4 shows the JSI of Ch1–Ch8, Ch2–Ch7, and Ch3–Ch6. It is seen that all three JSI spectrograms exhibit strong spectral correlation. The width of the ellipse, which is about 10 pm, depends on the linewidth of the pump and

the signal, and its accuracy is affected by the resolution of the measurement. The CW lasers have a linewidth of 11 pm. It is noticed that the antidiagonal ellipses are not rigorously symmetric, which is considered to arise from the slight temperature-drift-induced resonance shift. In general, the resolution of the JSI is controlled by both the laser and the OSA. Specifically, the resolution of the x axis is controlled by the signal laser, while the resolution of the y axis is related to the detected idler.

The spectral correlation of a photon-pair state is typically characterized by the Schmidt number, $K = 1/\sum_n \lambda_n^2$, where λ_n are the Schmidt magnitudes that are subject to the normalization, $\sum_n \lambda_n = 1$. The Schmidt magnitudes are obtained from a singular value decomposition of the joint spectral amplitude [26]. Generally, $K = 1$ indicates completely spectral uncorrelation, while $K > 1$ indicates spectral correlation. The Schmidt number represents how many frequency modes are correlated and reflects the number of degrees of freedom in a physical system; it corresponds to the number of independent communication channels between the sources and the receivers in a communication system [27,33].

In the measurement, K is calculated to be 20.7, 20.2, and 22.0 for Ch1–Ch8, Ch2–Ch7, and Ch3–Ch6, respectively. Because the JSA is calculated from the measured JSI, the lack of phase information means that the obtained values for K represent lower bounds [23].

K can also be estimated through the measurement of the unheralded second-order correlation function $g^{(2)}$, according to $K \approx 1/(g^{(2)} - 1)$ [34]. Based on the setup in Fig. 1(a), the signal arm is separated into two by a 50%/50% coupler, and then they are connected to the SPDs, individually. At 0-dBm pump power, $g^{(2)}$ for Ch8, Ch7, and Ch6 is measured as 1.047 ± 0.008, 1.047 ± 0.016, and 1.045 ± 0.012, corresponding to K values of 21.3, 21.3, and 22.2, respectively. As a quantum method, the unheralded second-order correlation function
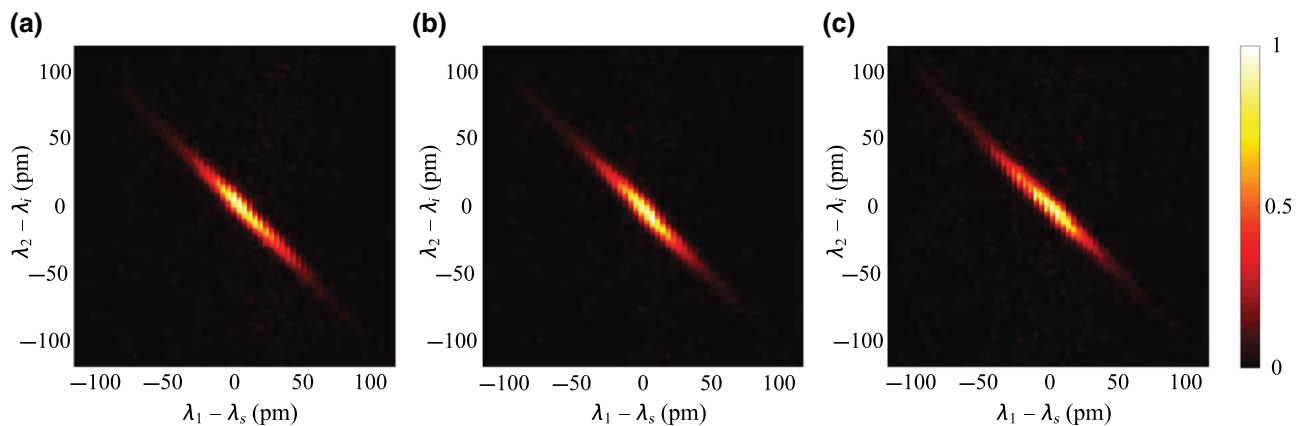

FIG. 4. The reconstructed JSIs for (a) Ch1–Ch8, (b) Ch2–Ch7, and (c) Ch3–Ch6. The horizontal axis is the signal wavelength range centered at the resonance wavelength, and the vertical axis is the corresponding idler wavelength range. λ_1 and λ_2 are the swept wavelength around the signal and idler resonance, respectively.

measurements have larger error bars, but the mean values still show a good agreement with the classical JSI measurement. Generally, the above experimental results reveal high and uniform degrees of quantum correlation in our multichannel system and show that every resonance pair in the system is able to support at least 20 spectral modes. Such a high Schmidt number indicates a high-dimensional correlated state. This multichannel system, as wavelength multiplexed heralded single-photon sources, has a profound potential to apply frequency correlation to high-dimensional encoding for parallel QKD, extending the capacity of the quantum network.

IV. CONCLUSION

In conclusion, we report a multichannel microring photon-pair system that is capable of generating photon pairs with a high-quality matching ITU frequency grid. We measure the JSI of the system by an OSA with a high resolution of 2 pm through stimulated four-wave mixing for better quantification of the Schmidt number. The high resolution has the potential to depict the JSI of ultrahigh-quality microring resonators with a narrow resonant bandwidth. Our generated photon pairs show strong and uniform spectral correlations, demonstrated by applying the classical method to a multichannel microring photon-pair source with high accuracy. The amount of spectral entanglement obtained by classical construction of the JSI shows good agreement with the measurement of unheralded second-order correlation. Consequently, our work demonstrates an efficient integrated photon-pair source for the potential application of frequency-encoded multichannel high-dimensional quantum key distribution, which becomes an attractive candidate for large-capacity quantum information processing as a quantum frequency comb.

ACKNOWLEDGMENTS

---

[1] P. Kok, W. J. Munro, K. Nemoto, T. C. Ralph, J. P. Dowling, and G. J. Milburn, Linear optical quantum computing with photonic qubits, Reviews of Modern Physics **79**, 797 (2007).

[2] D. A. Kalashnikov, Z. Pan, A. I. Kuznetsov, and L. A. Krivitsky, Quantum Spectroscopy of Plasmonic Nanostructures, Phys. Rev. X **4**, 355 (2014).

[3] G. B. Lemos, V. Borish, G. D. Cole, S. Ramelow, R. Lapkiewicz, and A. Zeilinger, Quantum imaging with undetected photons, Nature **512**, 409 (2015).

[4] J. Y. Hu, B. Yu, M. Y. Jing, L. T. Xiao, S. T. Jia, G. Q. Qin, and G. L. Long, Experimental quantum secure direct communication with single photons, Light Science & Applications **5**, e16144 (2015).

[5] M. Li, C. L. Zou, X. F. Ren, X. Xiong, Y. J. Cai, G. P. Guo, L. M. Tong, and G. C. Guo, Transmission of photonic quantum polarization entanglement in a nanoscale hybrid plasmonic waveguide, Nano Lett. **15**, 2380 (2015).

[6] A. Martin, F. Kaiser, A. Vernier, A. Beveratos, V. Scarani, and S. Tanzilli, Cross time-bin photonic entanglement for quantum key distribution, Phys. Rev. A. **87**, 020301 (2012).

[7] J. Nunn, L. J. Wright, C. Söller, L. Zhang, I. A. Walmsley, and B. J. Smith, Large-alphabet time-frequency entangled quantum key distribution by means of time-to-frequency conversion, Opt. Express **21**, 15959 (2013).

[8] Q. Zhang, H. Takesue, S. W. Nam, C. Langrock, X. Xie, B. Baek, M. M. Fejer, and Y. Yamamoto, Distribution of time-energy entanglement over 100 km fiber using superconducting single-photon detectors, Opt. Express **16**, 5776 (2008).

[9] A. Banerjee, Y. Park, F. Clarke, H. Song, S. Yang, G. Kramer, K. Kim, and B. Mukherjee, Wavelength-division-multiplexed passive optical network (wdm-pon) technologies for broadband access: A review, Journal of Optical Networking **4**, 737 (2005).

[10] A. Ciurana, V. Martin, J. Martinez-Mateo, B. Schrenk, M. Peev, and A. Poppe, Entanglement distribution in optical networks, IEEE J. Sel. Top. Quantum Electron. **21**, 6400212 (2015).

[11] D. Aktas, B. Fedrici, F. Kaiser, T. Lunghi, L. Labonte, and S. Tanzilli, Entanglement distribution over 150 km in wavelength division multiplexed channels for quantum cryptography, Laser Photonics Rev. **10**, 451 (2016).

[12] C. Reimer, L. Caspani, M. Clerici, M. Ferrera, M. Kues, M. Peccianti, A. Pasquazi, L. Razzari, B. E. Little, and S. T. Chu *et al.*, Integrated frequency comb source of heralded single photons, Opt. Express **22**, 6535 (2014).

[13] C. Xiong, B. Bell, and B. J. Eggleton, Cmos-compatible photonic devices for single-photon generation, Nanophotonics **5**, 427 (2016).

[14] C. Ma, X. Wang, V. Anant, A. D. Beyer, M. D. Shaw, and S. Mookherjea, Silicon photonic entangled photon-pair and heralded single photon generation with car > 12,000 and g(2)(0) < 0.006, Opt. Express **25**, 32995 (2017).

[15] K. Guo, E. N. Christensen, J. B. Christensen, J. G. Koefoed, D. Bacco, Y. Ding, H. Ou, and K. Rottwitt, High coincidence-to-accidental ratio continuous-wavephoton-pair generation in a grating-coupled silicon strip waveguide, Appl. Phys. Express **10**, 062801 (2017).

[16] J. E. Sharping, K. F. Lee, M. A. Foster, A. C. Turner, B. S. Schmidt, M. Lipson, A. L. Gaeta, and P. Kumar, Generation of correlated photons in nanoscale silicon waveguides, Opt. Express **14**, 12388 (2006).

[17] D. Grassani, S. Azzini, M. Liscidini, M. Galli, M. J. Strain, M. Sorel, J. E. Sipe, and D. Bajoni, Micrometer-scale integrated silicon source of time-energy entangled photons, Optica **2**, 88 (2015).

[18] K. Guo, X. Shi, X. Wang, J. Yang, Y. Ding, H. Ou, and Y. Zhao, Generation rate scaling: The quality factor optimization of microring resonators for photon-pair sources, Photon. Res. **6**, 587 (2018).

[19] J. A. Steidle, M. L. Fanto, C. C. Tison, Z. Wang, S. F. Preble, and P. M. Alsing, High spectral purity silicon ring resonator photon-pair source, Proc. SPIE. Int. Soc. Opt. Eng. **9500**, 950015 (2015).

[20] W. Bogaerts, P. De Heyn, T. Van Vaerenbergh, K. De Vos, S. K. Selvaraja, T. Claes, P. Dumon, P. Bienstman, D. Van Thourhout, and R. Baets, Silicon microring resonators, Laser Photonics Rev. **6**, 47 (2012).

[21] L. Caspani, C. Xiong, B. J. Eggleton, D. Bajoni, M. Liscidini, M. Galli, R. Morandotti, and D. J. Moss, Integrated sources of photon quantum states based on nonlinear optics, Light Sci. Appl. **6**, e17100 (2017).

[22] M. Liscidini and J. Sipe, Stimulated Emission Tomography, Phys. Rev. Lett. **111**, 193602 (2013).

[23] I. Jizan, L. G. Helt, C. Xiong, M. J. Collins, D.-Y. Choi, C. J. Chae, M. Liscidini, M. J. Steel, B. J. Eggleton, and A. S. Clark, Bi-photon spectral correlation measurements from a silicon nanowire in the quantum and classical regimes, Sci. Rep. **5**, 12557 (2015).

[24] B. Fang, O. Cohen, M. Liscidini, J. E. Sipe, and V. O. Lorenz, Fast and highly resolved capture of the joint spectral density of photon pairs, Optica **1**, 281 (2014).

[25] D. Grassani, A. Simbula, S. Pirotta, M. Galli, M. Menotti, N. C. Harris, T. Baehr-Jones, M. Hochberg, C. Galland, M. Liscidini, and D. Bajoni, Energy correlations of photon pairs generated by a silicon microring resonator probed by stimulated four wave mixing, Sci. Rep. **6**, 23564 (2016).

[26] I. Jizan, A. S. Clark, L. G. Helt, M. J. Collins, E. Mägi, C. Xiong, M. J. Steel, and B. J. Eggleton, High-resolution measurement of spectral quantum correlations in the telecommunication band, Opt. Commun. **327**, 45 (2014).

[27] R. Kumar, J. R. Ong, M. Savanier, and S. Mookherjea, Controlling the spectrum of photons generated on a silicon nanophotonic chip, Nat. Commun. **5**, 5489 (2014).

[28] Y. Ding, H. Ou, and C. Peucheret, Ultrahigh-efficiency apodized grating coupler using fully etched photonic crystals, Opt. Lett. **38**, 2732 (2013).

[29] K. Guo, L. Yang, X. Shi, X. Liu, Y. Cao, J. Zhang, X. Wang, J. Yang, H. Ou, and Y. Zhao, Nonclassical Optical Bistability and Resonance-locked Regime of Photon-pair Sources Using Silicon Microring Resonator, Phys. Rev. Appl. **11**, 034007 (2019).

[30] A. B. Matsko, A. A. Savchenkov, D. Strekalov, V. S. Ilchenko, and L. Maleki, Optical hyperparametric oscillations in a whispering-gallery-mode resonator: Threshold and phase diffusion, Phys. Rev. A. **71**, 033804 (2005).

[31] S. Azzini, D. Grassani, M. J. Strain, M. Sorel, L. G. Helt, J. E. Sipe, M. Liscidini, M. Galli, and D. Bajoni, Ultra-low power generation of twin photons in a compact silicon ring resonator, Opt. Express **20**, 23100 (2012).

[32] K. Guo, S. M. M. Friis, J. B. Christensen, E. N. Christensen, X. Shi, Y. Ding, H. Ou, and K. Rottwitt, Full-vectorial propagation model and modified effective mode area of four-wave mixing in straight waveguides, Opt. Lett. **42**, 3670 (2017).

[33] J. Pors, S. Oemrawsingh, A. Aiello, M. Van Exter, E. Eliel, and J. Woerdman, Shannon Dimensionality of Quantum Channels and its Application to Photon Entanglement, Phys. Rev. Lett. **101**, 120502 (2008).

[34] A. Christ, K. Laiho, A. Eckstein, K. N. Cassemiro, and C. Silberhorn, Probing multimode squeezing with correlation functions, New J. Phys. **13**, 033027 (2011).